IOP Conf. Series: Materials Science and Engineering **224** (2017) 012023 doi:10.1088/1757-899X/224/1/012023

A Quadtree-gridding LBM with Immersed Boundary for Two-dimension Viscous Flows

Jieke Yao[1, a], Wenliang Feng[1], Bin Chen[1], Wei Zhou[1] and Shikun Cao[1]

[1]Chengdu Aircraft Industrial (group) CO.LTD., 610092, Chengdu, China

[a] yjk1106@163.com

Abstract. An un-uniform quadtree grids lattice Boltzmann method (LBM) with immersed boundary is presented in this paper. In overlapping for different level grids, temporal and spatial interpolation are necessary to ensure the continuity of physical quantity. In order to take advantage of the equation for temporal and spatial step in the same level grids, equal interval interpolation, which is simple to apply to any refined boundary grids in the LBM, is adopted in temporal and spatial aspects to obtain second-order accuracy. The velocity correction, which can guarantee more preferably no-slip boundary condition than the direct forcing method and the momentum exchange method in the traditional immersed-boundary LBM, is used for solid boundary to make the best of Cartesian grid. In present quadtree-gridding immersed-boundary LBM, large eddy simulation (LES) is adopted to simulate the flows over obstacle in higher Reynolds number (Re). The incompressible viscous flows over circular cylinder are carried out, and a great agreement is obtained.

1. Introduction

Lattice Boltzmann method (LBM) is a mesoscopic method, which springs from the later of 1980s. It is used mainly in the low-speed flows, porous media flows, multiphase flows and so on. However, traditional LBM has serious limitations for uniform grids. Some flow regions for large gradient need more refined grids, so numerical efficiency for traditional LBM is limited. In order to improve computational accuracy, the application of un-uniform grids has been mentioned gradually.

For the un-uniform grids, Yu et al proposed multi-block grids which are non-overlapped each other exchange message by interface [1]. The special treatment is carried out for different blocks to ensure conservation of the mass and momentum. The spline interpolation is adopted in the information exchange for coarse grids to refined grids to eliminate spatial asymmetry. However, it is very difficult to apply the spline interpolation for irregular boundary in the overlapping between coarse grids and refined grids. Therefore, un-uniform quadtree grid is used generally in the LBM. The quadtree grid is a hierarchical data structure, and its algorithm is very simple. In the irregular refined-region, information processing in the overlapping is very easy.

Immersed boundary method (IBM) is proposed by Peskin in 1972, and it mainly simulates mutual deformation between fluid and object boundary [2]. The IBM is based on macroscopic equation, and it is used in LBM as a method treating boundary in 2002 [3]. However, force density is carried out by Hooke's law, direct forcing method or momentum exchange method in the traditional immersed boundary-lattice Boltzmann method (IB-LBM). Therefore, no-slip boundary flowing over obstacle condition can be satisfied approximately. The velocity correction method proposed by Shu et al in 2010 contains unknown force density, and it is obtained by corrected velocity [4]. No-slip boundary condition is applied in this equation solved, so the velocity correction method can guarantee no-slip

Content from this work may be used under the terms of the Creative Commons Attribution 3.0 licence. Any further distribution of this work must maintain attribution to the author(s) and the title of the work, journal citation and DOI.
Published under licence by IOP Publishing Ltd

boundary condition better than traditional IB-LBM. For the IB-LBM, the flow in higher Reynolds number (Re) can be simulated hardly. If the flow for higher Re is simulated by refining grids persistently based on enough grids, this will cause a large number of grids, low computing speed, unstable numerical calculation, and so on. And at the same time, the flow will transform from laminar flow to turbulence when the Re is higher. To solve turbulent flow, large eddy simulation (LES) is adopted in IB-LBM.

An un-uniform quadtree grids IB-LBM is proposed in present paper. Boundary processing technique and LES are introduced to carry out the flows over circle cylinder in this paper.

2. The briefing introduction of IB-LBM

Being different from traditional numerical model, LBM is a mesoscopic method, and it can describe basic physical properties of microscopic equation and keep macroscopic equation. Lattice Boltzmann equation is acquired by dispersion of continuous Boltzmann equation in temporal and spatial variation [5]. For the simulation of obstacle in the flow field, lattice Boltzmann equation containing force proposed by Guo et al [6] is used. The equation is listed as following:

$$f_a\left(x+e_a\delta t,t+\delta t\right)-f_a\left(x,t\right)=-\frac{1}{\tau}\left(f_a\left(x,t\right)-f_a^{eq}\left(x,t\right)\right)+F_a\delta t \tag{1}$$

$$F_a=\left(1-\frac{1}{2\tau}\right)w_a\left(\frac{\vec{e}_a-\vec{u}}{c_s^2}+\frac{\vec{e}_a\cdot\vec{u}}{c_s^4}\vec{e}_a\right)\cdot\vec{f} \tag{2}$$

$$\rho\vec{u}=\sum_a\vec{e}_a f_a+\frac{1}{2}\vec{f}\delta t \tag{3}$$

Where $\vec{x}$ is coordinate of Euler point in the flow field, $\vec{u}$ is the speed of fluid, ρ is the density of fluid, f_a is distribution function of particle, f_a^{eq} is corresponding equilibrium distribution function, τ is single relaxation time, $\vec{e}_a$ is discrete velocity of particle, w_a is weight coefficient, $\vec{f}$ is external force density acting on the fluid and F_a is the external force acting on the wall. In the D2Q9 model [7], the velocity of particle is shown in Figure 1.

$$\left[\vec{e}_0\ \vec{e}_1\ \vec{e}_2\ \vec{e}_3\ \vec{e}_4\ \vec{e}_5\ \vec{e}_6\ \vec{e}_7\ \vec{e}_8\right]=c\begin{bmatrix}0&1&1&0&-1&-1&-1&0&1\\0&0&1&1&1&0&-1&-1&-1\end{bmatrix} \tag{4}$$

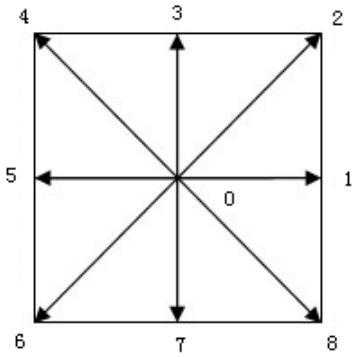


Figure 1. D2Q9 lattice model

Where $c=\delta x/\delta t$ (if $\delta x=\delta y=\delta t$, $c=1$), δx and δt are temporal step and spatial step respectively. Corresponding equilibrium distribution function is:

$$f_a^{eq}\left(\vec{x},t\right)=\rho w_a\left[1+\frac{e_a\cdot u}{c_s^2}+\frac{\left(e_a\cdot u\right)^2-\left(c_s\left|u\right|\right)^2}{2c_s^4}\right] \tag{5}$$

Where c_s is the sound speed of model, $c_s = c/\sqrt{3}$ and weight coefficient is $w_0 = 4/9$, $w_1 = w_2 = w_3 = w_4 = 1/9$ and $w_5 = w_6 = w_7 = w_8 = 1/36$. In this model, the relationship of τ and kinematic viscosity coefficient for the fluid is $\upsilon = (\tau - 0.5)c_s^2 \delta t$.

3. The generation and refinement of quadtree grids

Traditional LBM requires uniform and regular grids [8], but high-density grids are demanded in the large gradient flow region of or near the curved solid. Therefore, the application of traditional LBM is limited. In order to improve numerical efficiency and accuracy, Filippov et al proposed grid refinement technique [9, 10], so the use of un-uniform grid makes LBM get wide application.

Quadtree grid based on recursion and decomposition principle is a hierarchical data structure [11, 12]. Its data storage and adaptive grid refinement are very simple. Main unit of quadtree grid is quadtree unit. Very quadtree unit contains four grid nodes. These grids nodes store geometry information and physical quantity in the flow field, and all computing processes are done by these grid nodes. Quadtree grid has two types: root unit and leaf unit. Root unit is divided into four equal leaf unit. Very tree unit stores pointers of four grid nodes, leaf units and neighboring units. The process of grid refinement is shown in Figure 2.

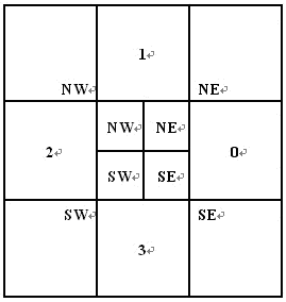


Figure 2. Refinement grid model

The process of grid generation is as follows:

- Firstly, rectangular region is used as bottom element, and it is divided into many quadtree grid units. Grid step of Very tree unit is unit length, and four vertexes are four grid nodes of quadtree unit. Four quadtree units on the left of it, on the right of it, above it and under it are neighboring units.
- Secondly, grid unit is divided by the controlling function or gradient of physical quantity for the nodes in the flow flied, and very quadtree unit is divided into four identical leaf units.

The grids refined to three levels by the controlling function is shown in Figure 3.

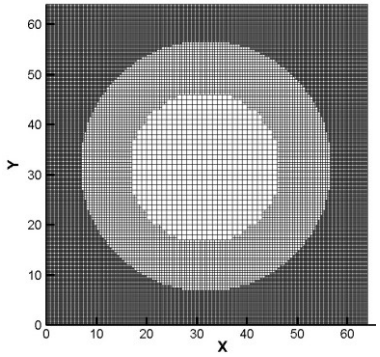


Figure 3. Quadtree grid in square domain with high grid density near the edge

In order to apply the quadtree grids refined at any boundary to the LBM, the present paper used the method in the reference [1] which presented that coarse grid and refined grid didn't have overlapping domain, and a smooth connection for the flow was guaranteed by information transfer, spatial interpolation and temporal interpolation on the overlap. However, the application of three spline interpolation in space is very difficult for the irregular refined region.

Because the four leaf units divided are identical in the quadtree grids, the spatial and temporal steps are equal in the same level grid. Equal interval interpolation in spatial and temporal aspects are adopted to replace Lagrange interpolation and three spline interpolation. This makes the LBM get more extensive application, and two order accuracy is guaranteed in spatial and temporal aspects.
Detailed implement steps of multi-levels grids refined for any boundary in the LBM is listed as follows: firstly, neighboring units are arranged by recursive algorithm for very leaf unit based on bottom unit. And the same time, the nodes of streaming and collision are marked in very level grid. Secondly, because the nodes for neighboring units are used in streaming, the streaming is done for grid units. In order to avoid repeating streaming for the same node, new marker is done for the node completing streaming until the streaming is finished in the same level grid. Then original markers are recovered for these. Thirdly, macroscopic calculation and collision are carried out at the nodes, so the two processes are done by the pointer in very level grids. Fourthly, according to the demand of multi-block grid, the streaming and collision for coarse grid are once, this process for refined grid is twice. And this process is circulated in the LBM computation.

4. The treatment of boundary condition

4.1. The boundary condition on the wall

For the treatment of the boundary on the wall, the velocity correction proposed by Wu and Shu [4] is adopted. In the velocity correction, $\vec{u}^*$ is intermediate velocity, and it is obtained by:

$$\rho\vec{u}^* = \sum_a \vec{e}_a f_a \ , \ \rho\delta\vec{u} = \frac{1}{2} f\delta t \tag{6}$$

then equation (3) can be written as $\vec{u} = \vec{u}^* + \delta\vec{u}$. Where $\delta\vec{u}$ is the correction velocity at Eulerian points. In the IB-LBM, the boundary of the object is represented by a set of Lagrangian points $\vec{X}_B(s_l,t)(l=1,2,\cdots,m)$. Here, we can set an unknown velocity correction vector δU_B^l at very Lagrangian points. The velocity correction $\delta\vec{u}$ at the Eulerian point can be obtained by the following Dirac delta function interpolation:

$$\delta\vec{u} = \int_\Gamma \delta\vec{U}_B\left(\vec{X}_B,t\right)\delta\left(\vec{x}-\vec{X}_B(s,t)\right)ds \tag{7}$$

The Dirac delta function is $\delta\left(\vec{x}-\vec{X}_B(s,t)\right) = D_{ij}\left(\vec{x}_{ij}-\vec{X}_B^l\right) = \delta\left(x_{ij}-X_B^l\right)\left(y_{ij}-Y_B^l\right)$. Where $\delta(r)$ is proposed by Peskin [13] as $\delta(r) = \frac{1}{4}\left(1+\cos\left(\frac{\pi|r|}{2}\right)\right)(if\ |r|\le 2)$ or $\delta(r)=0(if\ |r|>2)$. Using the Dirac delta function, the velocity correction at Eulerian points can be expressed as:

$$\delta\vec{u}\left(\vec{x}_{ij},t\right) = \sum_l \delta\vec{U}_B^l\left(\vec{X}_B^l,t\right)D_{ij}\left(\vec{x}_{ij}-\vec{X}_B^l\right)\Delta s_l \quad (l=1,2,\ldots,m) \tag{8}$$

And at the same time, the velocity correction at Lagrangian points can be obtained:

$$\vec{U}_B^l\left(\vec{X}_B^l,t\right) = \sum_{i,j}\vec{u}\left(\vec{x},t\right)D_{ij}\left(\vec{x}_{ij}-\vec{X}_B^l\right)\Delta x\Delta y \tag{9}$$

Substituting equation (8) and $\vec{u} = \vec{u}^* + \delta\vec{u}$ into equation (9) gives:

$$\vec{U}_B^l\left(\vec{X}_B^l,t\right) = \sum_{i,j}\vec{u}^*\left(\vec{x},t\right)D_{ij}\left(\vec{x}_{ij}-\vec{X}_B^l\right)\Delta x\Delta y + \sum_{ij}\sum_n\left[\delta\vec{U}_B^n\left(\vec{X}_B^n,t\right)D_{ij}\left(\vec{x}_{ij}-\vec{X}_B^n\right)\Delta s\right]D_{ij}\left(\vec{x}_{ij}-\vec{X}_B^l\right)\Delta x\Delta y \tag{10}$$

Equation system (10) can be further rewritten as the following matrix form:

$$AX = B \tag{11}$$

where $X=\left\{\delta\vec{U}_B^1,\delta\vec{U}_B^2,\ldots,\delta\vec{U}_B^m\right\}^T$, $B=\left\{\Delta u_1,\Delta u_2,\ldots,\Delta u_m\right\}^T$ with $\Delta u_l=U_B^l\left(X_B^l,t\right)-\sum_{i,j}u^*\left(x,t\right)\cdot D_{ij}\left(\vec{x}_{ij}-\vec{X}_B^l\right)\Delta x\Delta y \quad \left(l=1,2,\ldots,m\right)$.

Note that the elements of matrix A are only related to the boundary points and their nearby Eulerian points. The pressure at the Lagrangian points is calculated by $p=c_s^2\rho$. Therefore, the correction velocity at Eulerian points can be calculated by solving equation (11), the correction velocity at Lagrangian points can be obtained by equation (8).

4.2 The boundary condition in the far field

Because the far boundary has a smaller influence on the flow nearby the wall, the treatment for the far field boundary can use initial condition. However, the wake has a greater influence on the flow, so the treatment of right boundary in the x direction can use convective boundary condition proposed by Kim [14]:

$$\frac{\partial u}{\partial t}+U_0\frac{\partial u}{\partial x}=0 \tag{12}$$

where U_0 is the initial velocity of field, u is the velocity of field in the x direction.

5. The primary process of LBM and numerical experiments

5.1 Large eddy model

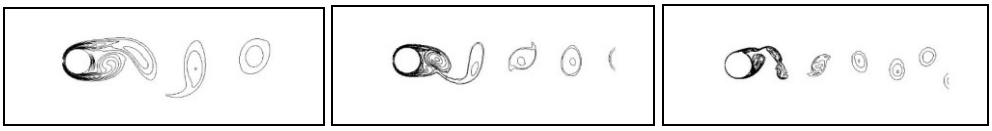
Because IB-LBM simulates mainly the flow at high Re, kinematic viscosity coefficient is very small (kinematic viscosity coefficient is inversely proportional to Re). According the relationship of τ and υ , relaxation time τ is c lose to 0.5. Therefore, distribution function of particle may be negative value. This may result in numerical instability. In order to solve this problem, LES proposed Hou and Sterling [15] is adopted. That combines IB-LBM with LES to solve the flow at higher Re. This method is based on standard Smagorinsky subgrid model [16], and its principle is that single relaxation time (SRT) for any node is different when they are colliding. Finally, the SRT can be obtained by formulation derivation as follows:

$$\tau=\frac{1}{2}\left(\sqrt{\tau_0^2+\frac{18}{\rho\delta t^2}C\Delta^2\sqrt{2Q}}+\tau_0\right) \tag{13}$$

Where τ_0 is the SRT without the LES Smagorinsky model, C is Smagorinsky constant and it is usually set to 0.1, Δ is filter scale and this value is usually spatial step, $Q=\overline{\Pi}_{ij}\overline{\Pi}_{ij}$, $\overline{\Pi}_{ij}=\sum\vec{e}_{ai}\vec{e}_{aj}\left(f_a-f_a^{eq}\right)$ is the non-equilibrium stress tensor and i , j are x and y direction respectively.

5.2 The numerical experiments

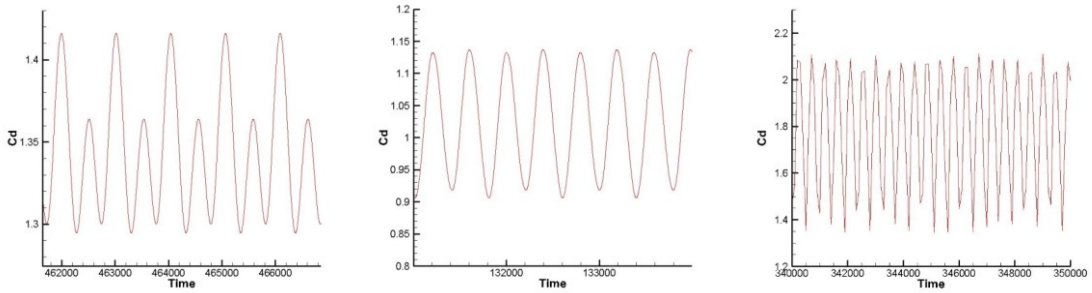
In this paper, the flows over circular cylinder are carried out to validate the methods of quadtree grids, the treatment of boundary and LES in the LBM. In the present simulations, the Re is defined as $\mathrm{Re}=(U_\infty D)/\upsilon$, the drag coefficient C_d and the Strouhal number St are defined as $C_d=F_d/(0.5\rho_\infty U_\infty^2 D)$, $St=(f_q D)/U_\infty$. Where U_∞ is the free stream velocity, ρ_∞ is the free stream density, D is the diameter of cylinder, F_d is the drag and f_q is the vortex shedding frequency. The drag is obtained by $F_d=-\frac{d}{dt}\left(\int_\Omega u_1 d\Omega\right)-\int_s\left[u_1\vec{u}\cdot\vec{n}+pn_1-\mu\left(\frac{\partial u_1}{\partial x_i}+\frac{\partial u_i}{\partial x_1}\right)\right]ds$. Where s the control surface, $\vec{n}$ the normal vector of control surface, and the subscripts 1 and 2 stand for the x direction and y direction respectively. The instantaneous vorticity is shown in Figure 4.



(a) Re=200 (b) Re=1000 (c) Re=3900

Figure 4. Vorticity contours for different Reynolds number

From seen the figure 4, the stable symmetric vortex behind the cylinder appears when the Re is much lower. However, the vortex shedding occurs when the Re is much higher. Because may lead to the periodic oscillation for the drag, the figure 5 gives the variation of drag coefficient according to time. Figure 6 gives instantaneous streamline for Re=3900.



(a) Re=200 (b) Re=1000 (c) Re=3900

Figure 5. The variation of drag coefficient according to time

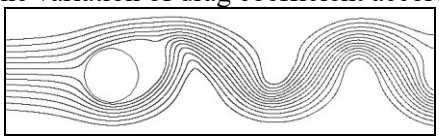


Figure 6. The instantaneous streamline for flow over a cylinder at Re=3900

The comparisons of mean drag coefficient $\overline{C}_d$ and Strouhal number St are listed in table 1.

Table 1. The mean drag coefficient and Strouhal numbers for different Reynolds number

Re	Method	$\overline{C}_d$	St
200	Finite-element method and N-S equation [17]	1.35	0.196
	A Fractional Step Method[18]	1.3	0.196
	The Present method	1.36	0.196
1000	Stanley K.Jordan al[19]	1.24	0.206
	Finite-element method and N-S equation [17]	1.47	0.234
	The Present method	1.03	0.227
3900	LBM-LES2D[20]	1.827	0.225
	Finite-element method[21]	1.74	0.263
	The Present method	1.74	0.226

In Figure 6, because no-slip boundary based on velocity correction method stops fluid penetration, the streamlines around the cylinder round cylindrical surface. And at the same time, the streamline can smooth transition in different level, which is because information processing for interface between coarse mesh and refined mesh is appropriate to guarantee smooth transition of fluid. However, the essential cause is that numerical error is much smaller in the interpolation, which shows that the precision for equal interval interpolation in present paper dovetail nicely with the precision of LBM. Table 1 shows that the higher for Re, the greater for Strouhal number, which indicates the faster vorticity is shedding. A great agreement with literature is obtained in the table 1, but a small error is going on. That is due to the section of parameters in the model, such as the section of control domain, the section of computational domain, the method of interpolation, and so on.

6. Conclusion

Firstly, the quadtree-gridding refinement which allots the neighbors of leaf units and marks the nodes of streaming and collision in different level mesh is applied in the LBM for multi-level refinement of arbitrary boundary. Equal interval interpolation in temporal and spatial space is used in the different

grid interface, and this method is simpler than three spline interpolation and Lagrange interpolation. Because the temporal and spatial space is equal in the same grid level, the present method has the second order accuracy which matches the accuracy of LBM in the temporal and spatial direction. Secondly, the velocity correction method is adopted in immersed boundary, which ensures the non-slip boundary compared to the boundary treatment technique in the traditional IB-LBM. Thirdly, the LES is applied to the present IB-LBM to simulate the flows with high Re around the obstacle. Lastly, the flows is simulated for the different Re to validate the present method, and the results agree well with those of other methods.

References

[1] D. Z. Yu, R. W. Mei, W. Shyy, A multi-block lattice Boltzmann method for viscous fluid flows[J]. International journal for numerical methods in fluids, 2002, 39(2): 99-120.
[2] C. S. Peskin, Flow patterns around heart valves: a numerical method[J]. Journal of Computational Physics, 1972, 10(2): 252-271.
[3] Z. G. Feng, E. E. Michaelides, Hydrodynamic force on spheres in cylindrical and prismatic enclosure[J]. Journal of Multiphase Flow, 2002, 28(3): 479-496.
[4] J. Wu, C. Shu, Y. H. Zhang, Simulation of incompressible viscous flows around moving objects by a variant of immersed boundary-lattice Boltzmann method[J]. International Journal for Numerical Methods in Fluids, 2010, 62(3): 327-354.
[5] X. He, L. S. Luo, Theory of the lattice Boltzmann method: from the Boltzmann equation to the lattice Boltzmann equation[J]. Physical Review E, 1997, 56(6): 6811-6817.
[6] Z. Guo, C. Zheng, B. Shi, Discrete lattice effects on the forcing term in the lattice Boltzmann method[J]. Physical Review E., 2002, 65(4): 046308.
[7] Y. H. Qian, D. d'Humieres, P. Lallemand, Lattice BGK model for Navier-Stokes equation[J]. Europhysic Letters, 1992, 17(6): 479-484.
[8] S. Chen, G. D. Doolen, Lattice Boltzmann method for fluid flows[J]. Annual review of fluid mechanics, 1998, 30(1): 329-364.
[9] O. Filippova, D. Hanel, Grid refine for lattice-BGK model[J]. Journal of Computational Physics, 1998, 147: 219–228.
[10] C. L. Lin, Y. G. Lai, Lattice Boltzmann method on composite grids[J]. Physical Review E, 2000, 62(2): 2219-2225.
[11] H. Samet, Applications of Spatial Data Structures [M]. Addison-Wesley, MA, 1990.
[12] H. Samet, Neighbor finding techniques for images represented by quadtrees [J]. Computer Graphics and Image Processing, 1982, 18(1): 37-57.
[13] C. S. Peskin, The immersed boundary method[J]. Acta Numerica, 2001, 11: 479-517.
[14] D. H. Kim, K. S. Yang, M. Senda, Large eddy simulation of turbulent flow past a square cylinder confined in a channel[J]. Journal of Computational Physics, 2004, 33(1): 81-96.
[15] S. Hou, J. Sterling and S. Chen et al, A lattice Boltzmann subgrid model for high Reynolds number flows[J]. Pattern formation and lattice gas automata, 1994, 9401004(6): 151-166.
[16] Y. L. He, Y. Wang, Q. Li, Lattice Boltzmann method and its application[M]. Beijing: Science Press, 2008.
[17] K. Herfjord, A study of two-dimensional separated flow by a combination of the finite element method and N-S equations[D]. Norwegian Institute of Technology, 1996.
[18] J. R. Meneghini, F. Saltara, C. L. R. Siqueira, J. A. Ferrari. Numerical simulation of flow interference between two circular cylinders in tandem and side-by-side arrangements[J]. Journal of Fluids and Structures 2001, 15(2): 327-350.
[19] S. K. Jordan, J. E. Fromm, Oscillatory drag, lift, and torque on a circular cylinder in a uniform flow[J]. Physics of Fluids, 1972, 15(3): 371-376.
[20] A. G. Kravchenko, P. Moin, Numerical studies flow over a circular cylinder at ReD=3900[J]. Phycics of Fluids, 2000, 12(2): 403-417.
[21] P. Beaudan, P. Moin, Numerical experiments on the flow past a circular cylinder at sub-critical Reynolds number[R], Report No. TF-62, Department of Mechanical Engineering, Stanford University, 1994.